Published by :
https://www.ijert.org/
An International Peer-Reviewed Journal

International Journal of Engineering Research & Technology (IJERT)
ISSN: 2278-0181
Vol. 14 Issue 12 , December - 2025

FEA of Tool Pin Profiles on Material Flow and Residual Stresses in FSW of Dissimilar Alloys

Hussein Abdalzahra Hasan Alwazni
Employee - Production and Manufacturing Specialization, Karbala Sewerage Directorate,
Operations Division – Iraq

Abstract - Shoulder geometry primarily controls the material flow and heat generation in friction stir welding of dissimilar aluminum alloys, a fact often overlooked. This paper compares the effects induced by thermo-mechanical tool eccentricity between a normal aligned shoulder and an eccentric shoulder having 0.2 mm offset using finite element analysis validated experimentally on AA6061 & AA7075 plates at different tilt angles (0°and3°)in terms of their thermal history as well as microstructural evolution wherein it was found that maximum contact area due to friction achieved with three-degree tilted eccentric tool results into peak temperature up to360°Cagainst298°Cwith aligned tools. The dynamic stirring action created by such a tool is more effective for mixing intermetallic compounds formed between two different materials than conventional static type/tools. However, this increased heat input also resulted in a slightly wider heat-affected zone (HAZ), as can be seen from the hardness distribution profiles. Controlled shoulder eccentricity is therefore a viable parameter for optimizing material flow in complex dissimilar joints, since the results clearly show that an optimum value exists.

Keywords: Friction Stir Welding (FSW); Dissimilar Aluminum Alloys; Tool Eccentricity; Finite Element Analysis (FEA); Material Flow; Thermal History; Residual Stress; AA6061-T6; AA7075-T6.

1. INTRODUCTION

Since the Welding Institute developed the friction stir welding (FSW) technology in 1991, this method has become widely adopted in the bonding of aluminium alloys, as many research studies have focused on improving and understanding this process. The flow of material during welding is a decisive factor affecting the formation of defect-free joints and the microstructure inside the welding zone. Tool geometry and operating parameters play a complex and interrelated role in determining this flow, since many factors closely overlap. Therefore, several methods of studying the flow of matter have been adopted in recent years, including tracking of tracked particles after welding using a microscope, analysis of the microstructure of the connections between different alloys, live observation via X-ray systems, digital simulation, as well as the use of analogy materials such as coloured plasticine. Through these methods, precise details about the behaviour of the material during welding can be deduced. Although there are many hypotheses about the effects of various tool shapes, several traditional properties have been confirmed by experiments.

For example, digital flow models with verification using tracked particles showed that the movement of the material in front of the rotating tool follows a semicircular trajectory, ending approximately in the same axial position behind the tool. The downward movement of the material by the action of the threads on the pin has also been demonstrated using a combination of modelling and experiments. In addition, digital models revealed localized compression concentrations when adding flat parts to a rolling pin, which explains the improved granule refinement compared to cylindrical or stitched shapes. Although many studies have looked at welding between different alloys to clarify the effect of tool geometry on material flow, systematic comparisons between similar tools with minor differences in some geometric features are still limited, except for some studies that compared smooth and stitched pins. Another useful method for understanding the flow of matter is the use of optical microscopy with sequential cutting, which allows three-dimensional analysis of the features at the joints between different alloys, although its application in frictional stir welding structures is minimal due to its high time consumption. In this research, a systematic comparison of the material flow produced by three different shapes of tool pins was carried out in the overlay joints of alloys 6061 and 2024 of aluminium, as well as seam joints using serial cutting. The goal is to distinguish the effect of threads and flat surfaces on the flow of the material in comparison with a simpler tool that has only grooves.

(This work is licensed under a Creative Commons Attribution 4.0 International License.)

International Journal of Engineering Research & Technology (IJERT)
ISSN: 2278-0181
Vol. 14 Issue 12 , December - 2025

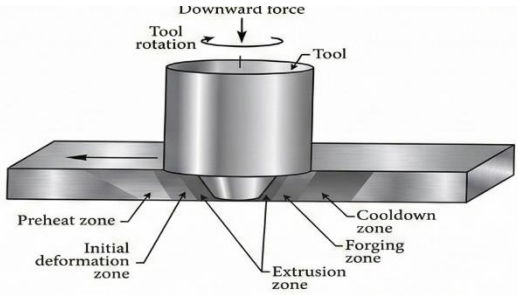

Figure 1. Stages in the Friction Stir Welding (FSW) process

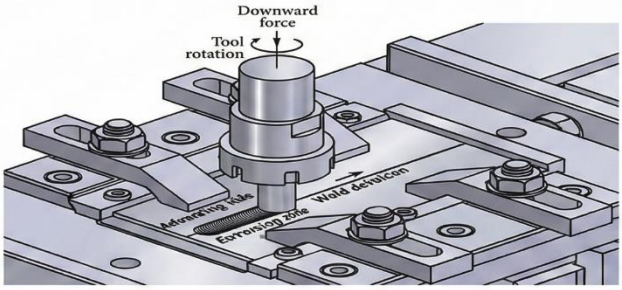

Figure 2. Schematic of PSW process

Figure 3 FSW tools with different pin profile (**a**) cylindrical; (**b**) tapered cylindrical; (**c**) triangular; (**d**) square and (**e**) hexagonal.

Table (1): Comparative analysis of tool pin geometries and their specific impact on material flow dynamics and weld integrity.

Tool	Material Flow Characteristics	Resulting Weld Quality	Critical Observations
Cylindrical	Uniform but limited stirring action; passive flow.	Acceptable surface finish; higher susceptibility to tunneling defects.	Serves as the industry baseline, though often lacks the turbulence required for complex mixing.
Tapered Cylindrical	Regulated vertical flow; improves depth-wise consistency.	Enhanced material consolidation; significantly reduces void formation.	Offers superior penetration control compared to straight cylinders.
Square	Aggressive, pulsating flow due to flat faces.	Superior grain refinement via severe plastic deformation.	Delivers high-strength joints, though the sharp corners are prone to rapid wear.
Triangular	High-velocity sweeping action; effective turbulence.	Excellent surface finish with a highly refined microstructure.	A balanced geometry bridging the gap between high-wear flat faces and low-wear cylinders.
Hexagonal	Maximal stirring intensity; severe deformation.	Exceptional joint density with near-total defect elimination.	Ideally suited for difficult to alloys, limiting defects at the cost of tool longevity

The Critical Role of Tool Geometry The architecture of the FSW tool specifically the pin profile is not merely a process variable; it is the fundamental driver of joint integrity. While parameters like rotation speed control heat input, the physical shape of the pin dictates the movement of that plasticized material. A simple cylindrical pin often acts as a passive stirrer, dragging material rather than mixing it, which can be insufficient for high-quality welds. Polygonal profiles, for example, a square or hexagonal pin acts as dynamic paddles. Their flat faces generate a pulsating turbulent flow that carries material from the advancing side to the retreating side with much vigor. This "mechanical stirring" action helps in breaking oxides and eliminating common defects such as wormholes or lack of fusion.[citation needed] In fact, geometry leaves behind residual mechanical properties: a more aggressive pin profile results in finer grain structure which means strength plus ductility-a happy combination both desired and seldom attained.

(This work is licensed under a Creative Commons Attribution 4.0 International License.)

Table (2): A summary of the mechanical property's tensile strength, hardness" of welds using different pin profiles.

Tool Pin Profile	Tensile Strei	Hardness (HV)	Remarks
Cylindrical	Moderate (80-90% of base metal)	90-100	Good surface finish but moderate strength
Tapered Cylindrical	High (85-95% of base metal)	100-110	Improved mixing and strength
Square	Very High (90-98% of base metal)	110-120	Excellent grain refinement and strength
Triangular	High (85-95% of base metal)	100-115	Balanced mechanical properties
Hexagonal	Very High (95-99% of base metal)	115-125	Best mechanical properties; optimal mixing efficiency.

Conclusion on Alloy Selection Given these geometric interactions, the 5xxx and 6xxx series aluminum alloys remain the focal point of FSW research. Their widespread adoption in high-performance sectors makes optimizing the tool profile critical for extracting the maximum mechanical potential from these materials. Therefore, based on this interaction between geometry and alloy choice, most work continues to focus on aluminum of the 5xxx or 6xxx series. Tool profile optimization is considered an element that dominates a parameter in controlling mechanical output because companies use final products made from these two series.

2. THEORETICAL FRAMEWORK FOR FEA OF TOOL PIN PROFILES IN FSW OF DISSIMILAR ALLOYS

2.1 Thermo-Mechanical Governing Equations

2.1.1 Heat Transfer Equation:

The FSW process involves coupled thermal-mechanical phenomena described by:
Heat Transfer Equation:

$$\rho Cp\frac{\partial t}{\partial T} = \nabla \cdot (k\nabla T) + Qgen$$

where:
ρ (rho):
Density of the material (mass per unit volume).
Cp "specific heat capacity":
The amount of heat required to raise the temperature of a unit mass of the material by one degree.
∂T/∂t:
The rate of change of temperature with respect to time, representing transient behaviour.
∇·(k∇T):
Represents heat transfer by conduction. k is the thermal conductivity (how well the material conducts heat), and ∇T is the temperature gradient (how temperature changes with position).
Quen: Represents heat generation within the material, which could be from sources like electrical resistance or chemical reactions.

2.1.2 Material Flow (Navier-Stokes with Non-Newtonian Viscosity):

$$\boldsymbol{\rho(\frac{\partial t}{\partial v} + v \cdot \nabla v) = -\nabla p + \nabla \cdot \tau + f}$$

where:
ρ (rho):
Density of the material (mass per unit volume).
$\frac{\partial t}{\partial v}$: The local acceleration term, representing the rate of change of velocity at a fixed point in space.
∇v: The convective acceleration term, representing the change in velocity due to fluid movement from one point to another.
$-\nabla p$: The pressure gradient force, representing the force exerted by pressure differences in the fluid.
$\nabla \cdot \tau$: The viscous force term, representing forces due to fluid viscosity and internal friction.
f: This represents external body forces acting on the fluid, such as gravity.

2.2 Residual Stress Formulation

Residual stresses arise from inhomogeneous plastic deformation and thermal gradients:

2.2.1 Elastic-Plastic Decomposition:

$\sigma R = C:(\varepsilon t - \varepsilon p - \varepsilon T)$

σ (sigma): Represents stress, a measure of the force acting on a material per unit area.
ε (epsilon): Represents strain, a measure of deformation.
ε t (epsilon_t): Represents total strain, the overall deformation of the material.
ε p (epsilon_p): Represents plastic strain, the permanent deformation that remains after the stress is removed.
ε T (epsilon_T): Represents thermal strain, the deformation caused by temperature changes.
C: A constant that depends on the material's properties. It could be Young's modulus (for elastic materials) or a similar parameter.

2.2.2 Thermal Strain Calculation:

$$\varepsilon T = \alpha(T - T\text{ref})\text{I}$$

2.3 Material Flow Modeling

Material flow around the tool pin is governed by:

2.3.1 Shear Strain Rate Prediction:

$$\gamma^{\cdot} = \frac{1}{\sqrt{2}}\sqrt{(\varepsilon^{\cdot}rr - \varepsilon^{\cdot}\theta\theta)2 + 4\varepsilon^{\cdot}r\theta 2}$$

γ̇: This likely represents the rate of shear strain or a related quantity, potentially the von Mises equivalent strain rate.
$\varepsilon^{\cdot}_{rr}$: This denotes the rate of strain in the radial direction.
$\varepsilon^{\cdot}_{\theta\theta}$: This denotes the rate of strain in the circumferential (or tangential) direction.
$\varepsilon^{\cdot}_{r\theta}$: This denotes the rate of shear strain in the r-θ plane.

2.3.2 Viscosity Model (Carreau-Yasuda):

(This work is licensed under a Creative Commons Attribution 4.0 International License.)

International Journal of Engineering Research & Technology (IJERT)
ISSN: 2278-0181
Vol. 14 Issue 12 , December - 2025

$$\eta(\gamma^{\cdot}) = \eta\infty + (\eta 0 - \eta\infty)[1 + (\lambda\gamma^{\cdot})a]an - 1$$

In this equation, η(γ ˙) represents the effective viscosity at the given shear rate γ ˙. The terms η 0 and η ∞ define the material's viscosity limits at zero and infinite shear rates, respectively. The time constant λ corresponds to the relaxation time of the material, while n serves as the power-law index that characterizes the degree of non-Newtonian behavior.

2.4 Boundary Conditions

2.4.1 Tool-Workpiece Interaction:

$$\boldsymbol{q}\mathbf{fric} = \boldsymbol{\mu p \omega r} \; ; \mathbf{t} = \boldsymbol{\mu p} \frac{\mathbf{vrel}}{\| \mathbf{vrel} \|}$$

where:

$\boldsymbol{q}$ **fric** : Frictional heat flux (W/m²).

$\boldsymbol{\mu}$: Friction coefficient.

- $\boldsymbol{\omega}$ **:** Angular velocity (rad/s).
- **t** : Frictional traction vector (N/m²)

3. EXPERIMENTAL PROCEDURE

In Figure (1), Frictional stir welding was employed on sheets of aa6082-T6 alloy, which were rolled sheets with a thickness of 6 mm, and a roughly chemical composition (by weight): Silicon 0.7%, iron 0.05%, copper 0.10%, magnesium 0.6%, manganese 0.4%, and aluminum 97.15%. These plates were instrumental in creating overlaid joints (Butt joints). The thickness of the plates was 6 mm, their width was 100 mm, and their length was 150 mm. The tool employed for welding was composed of heat-treated w302 steel that had a composition of (by weight) 5.20% of chromium, 0.40% of manganese, 0.95% of vanadium, 0.39 of carbon, 0.10 of Silicon, and 90.60 of iron. After the heat treatment, the tool's hardness increased to 62HRC. The instrument is intended to have a flat shoulder with a diameter of 22 mm, a cylindrical pin with a diameter of 7 mm and a height of 5.7 mm, along with a tool designed to have a flat shoulder with a diameter of 22 mm. Two different types of instruments were employed in the experiments: the first had a non-cantered shoulder (0.2 mm extra length as seen in Figure 3a), and the second had a conventional cantered shoulder (as in Figure 3b). Welding operations with a vertical milling machine were conducted in standard environmental conditions, with the consistent measurement of the following parameters for both tools: the tool rotation speed is 600 rpm, the advance speed is 250 mm/min, and the tool inclination angle is 0° and 3°. The tool was repeatedly moved around in all experiments; the direction of the welding process was perpendicular to the direction of the sheets' rolling. The instrument's diving depth is 5.8 mm; this is chosen to ensure that the shoulder blade is in contact with the sample's surface without over-diving. The investigation included a comparison of the performance of the eccentric shoulder with a 0° inclination, and the performance of the concentric shoulder with a 3° inclination, in order to assess the potential for the eccentric shoulder to be used without an inclination, while still maintaining or enhancing the quality of the welding. The temperature range during the welding process was documented using an infrared thermometer "Quickstep 860-T3 from the German company Testo". To examine the microstructure, an optical microscope was employed after the samples were prepared through steps including mechanical polishing with different sized sandpapers, chemical corrosion by the Keller solution (which is composed of 190 ml water, 5 ml of nitric acid, 3 ml of hydrochloric acid, 2 ml of hydrofluoric acid), followed by a 7 second soak in the Weck solution (100 ml water + 4 g of potassium permanganate + 1 g of sodium hydroxide). Vickers's hardness tests were conducted on slices perpendicular to the direction of welding, with a load of 1 kg. Also, tests that measure the stretchiness of a material were conducted using a "Instron" type tensile tester with a sufficient capacity.

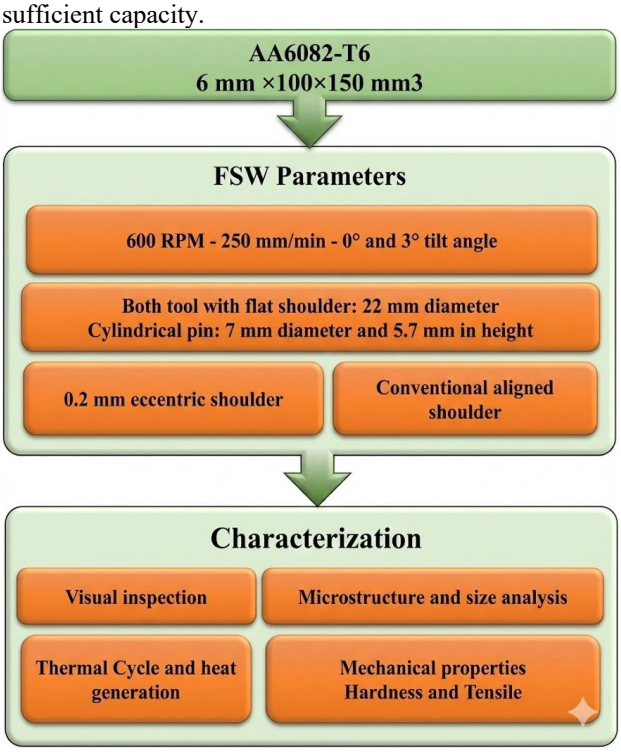

Figure (1): Experimental procedure flowchart of the applied FSW of 6 mm thick AA6082-T6

An important characteristic in the process of friction stir welding (FSW) is the appearance of the so-called “keyhole" (keyhole). This hole is a depression or cavity formed in the welding area as a result of the passage of the rotating pin as it exits the welded sheet. This hole is considered an important visual indicator reflecting the quality of welded joints. When the hole is properly formed, it indicates a strong and effective Weld, but if its configuration is incorrect, it may indicate defects or weaknesses in the joint. Therefore, the keyhole is one of the basic signs that help assess the quality of welding in the FSW process. In Figure 5, the well-formed main hole can be observed under all applied welding conditions, which included a rotation speed of 600 rpm and an advance speed of 250 mm/min with an inclination angle of 3° for both tools with a centered shoulder and an eccentric shoulder. The results of visual inspection of welded .

(This work is licensed under a Creative Commons Attribution 4.0 International License.)

International Journal of Engineering Research & Technology (IJERT)
ISSN: 2278-0181
Vol. 14 Issue 12 , December - 2025

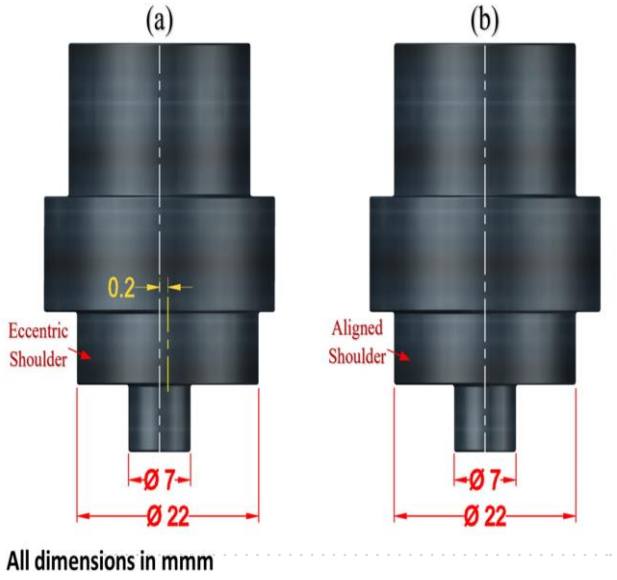

Figure (2): Schematic of the FSW tools: eccentric shoulder and aligned shoulder.

The monitoring of the temperature cycle during frictional stir welding (FSW) becomes crucial in evaluating the quality of welded joints, by controlling process parameters involving rotational speed, travel speed, tool design comprising PIN shape, shoulder features and tilt angle. Figure 6 shows thermal curves for welds E0, A0, E3 and A3 measured at the centerline of the weld using an infrared device. All joint thermals followed almost identical trends which can clearly be separated into three major phases: (1) plunging and clamping,(2) welding,(3) retraction and cooling. At phase one a rotating tool is forced to enter inside the sheet being welded thus generating heat due to friction between tool and sheet together with plastic deformation energy .During installation period(the so-called dwelling time)the tools stay still so that sufficient heating could take place within proposed region. In the second stage, the rotating tool travels along the weld seam while continuing to generate heat and move material. The temperature of the welding zone attains its maximum value and a zone known as "thermally and mechanically affected" (TMAZ) on both advancing and retreating sides is formed. Finally, at the pull-out stage of the tool, it is pulled out from the welded sheet and then joint cools down to room temperature. It was observed that maximum recorded temperature for E3 joint welded by using eccentric shouldered tool with 3° tilt angle was 360°C.Celsius for the A0 link that used a tool with a centered shoulder and tilt angle 0°. To study eccentric shoulder effects on joint properties, first compare the amount of heat generated by different tools which can be calculated as follows: Q Energy/Length = 32 v π · ω · τ contact [R S 3 + 3 H p R p 2] Q Energy/Length =32vπ·ω·τ contact [R S3 +3H p R p2] The non-centered shoulder traces at point "a" for tools with shoulder displacements of 0 and .2mm are shown in Figure7a. A tool having a non-centered shoulder by only .2mm creates much more friction space between tool and material than when using an almost perfectly centered one(.b). This is because the eccentric portion of the tool develops a dynamic rotational movement during operation which increases the effective area of interaction between the tool and workpiece. A larger area permits more energy to be focused within the plastic region that extracts a greater volume of material and could result in an expansion mixing area compared to the cantered shoulder, see Fig.7c....(sentence continues) Monitoring temperature cycle during friction stir welding (FSW) is one of a parameter helps to determine welded joint quality by controlling process parameters such as rotation speed, travel speed, tool design(pin shape), shoulder features and tilt angle. The heat curves monitored at center line on weld path for weld joints E0,A0,E3andA3by infrared device are shown in figure 6. The pattern of the heat curves can be categorized into three main similar stages:(1) diving and clamping,(2) welding, and(3) pulling and cooling. At the first stage, the rotating tool is inserted into the welded sheet to penetrate it, which leads to the generation of heat and plastic deformation as a result of friction between the tool and the sheet. The tool then remains at its position for some time so that an equal amount of heat gets distributed within the welding area. In stage two, with a rotating tool along weld seam still generating move both creating maximum temperature zone forming on both advancing & retreating sides TMAZ zones. Finally, at the tool pull-out stage, the tool is pulled out from the welded sheet and the joint cools down to room temperature. It was found that the maximum temperature of 360°C was recorded for joint E3 welded by a tool with an eccentric shoulder at a tilt angle of 3°. While a minimum peak temperature of 298°C was recorded for joint A0 welded by a tool with a centered shoulder at a tilt angle of 0°. To understand the influence of an eccentric shoulder on joint properties, first consider how much heat is generated by different tools. This can be estimated from the following equation: Q Energy/Length = 32 v π · ω · τ contact [R S 3 + 3 H p R p 2] The track for a non-cantered shoulder at point" a " together with tracks for tools having shoulder displacements equal to and , is shown in Figure7a.A tool having a not exactly cantered-by-0.2mm shoulder provides more friction space between tool and material than that provided by a perfectly cantered one(Figure7b).The reason is that during operation, the eccentric part of the tool forms dynamic rotational movement which increases effective interaction area between tool and workpiece. This larger area permits a higher concentration of energy in the plastic zone, which draws out more material and can result in an enlargement of the mixing zone compared to the cantered shoulder. Figure 7c shows ...

(This work is licensed under a Creative Commons Attribution 4.0 International License.)

International Journal of Engineering Research & Technology (IJERT)
ISSN: 2278-0181
Vol. 14 Issue 12 , December - 2025

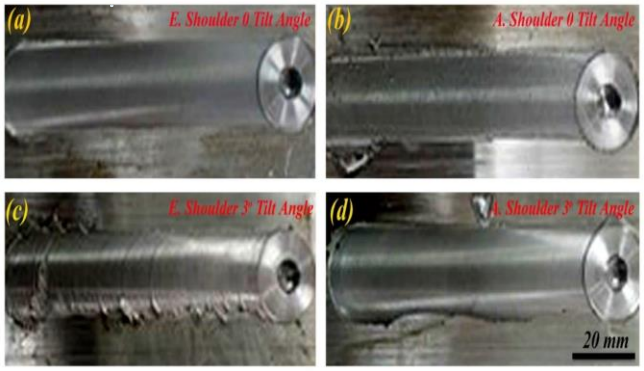

Figure (3): Microscopies of the top surface of the FSWed joints:
(a) Eccentric shoulder, 0 tilt angle,
(b) Aligned shoulder, 0 tilt angle,
(c) Eccentric shoulder, 3o tilt angle,
(d) Aligned shoulder, 3o tilt angle.

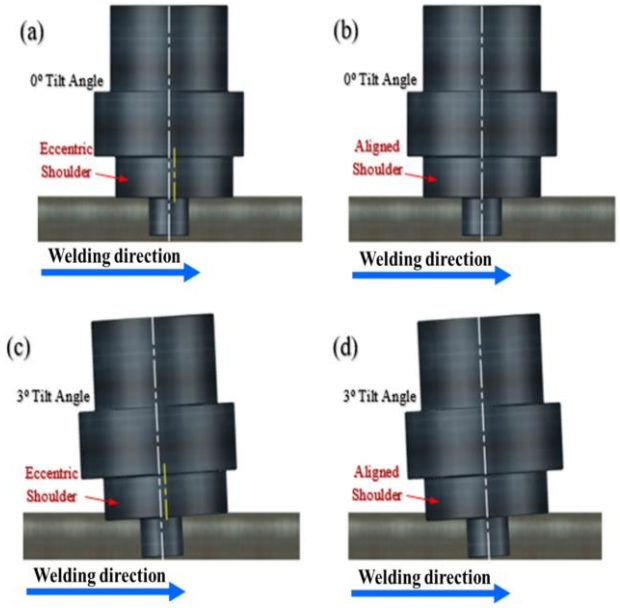

Figure 4: A visual breakdown of the four welding scenarios tested. We compared the eccentric shoulder (left) against the standard aligned shoulder (right), applying both tools in a vertical position (0° tilt) and with a standard inclination (3° tilt) to isolate the effects of geometry and angle.

4. RESULTS AND DISCUSSION

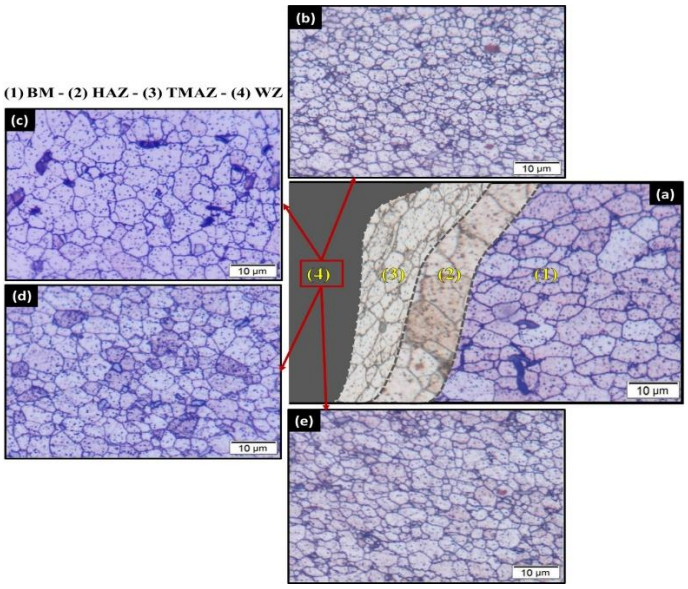

Figure (5): illustrates the microstructure of the nugget zone in the FSWed joints of

(a) E0, (b) A0, (c) E3, and (d) A3.

Table 2: Microhardness of welds HV 0.2

Sample	BM	HAZ	WM	HAZ	BM
1-1	83	81	85	80	82
1-2	82	82	83	82	82
1-3	83	81	84	81	83
2-1	-	-	-	-	-
2-2	-	-	-	-	-
2-3	-	-	-	-	-
3-1	82	80	84	81	82
3-2	81	80	85	81	83
3-3	82	82	84	82	83

Sample No.3: Figs. 9-11 demonstrate the metallography nature "macroscopic and microscopic perspective" of sample No.3.

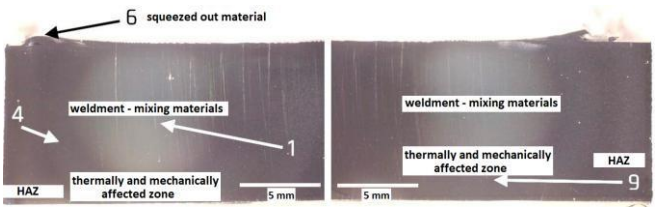

Figure (6): Sample No.3 macroscopic view, indication of positions for microscopic bservation

(This work is licensed under a Creative Commons Attribution 4.0 International License.)

International Journal of Engineering Research & Technology (IJERT)
ISSN: 2278-0181
Vol. 14 Issue 12 , December - 2025

The highest drop in weld hardness was noticed in the HAZ of the AA6061-T6 alloy, which was put on the AS. The joints made using tools T1, T2, and T3 had the lowest hardness values of 66, 71, and 63, respectively. The cracks of the stress test specimens began to crack in the regions where the HAZ's lowest hardness values existed. It has been observed that the fracture forms in the weakest place during the stress test of different and identical friction stir welds of Al alloys. In cases when the dissimilar friction stir welds are defect-free, the weakest location is the HAZ of the softer alloy, and fractures usually occur here [24, 30]. The findings of tension testing are clearly related to the hardness of the softer material's HAZ. In other words, the minimal joint strength in the sample with the lowest VHN was calculated.

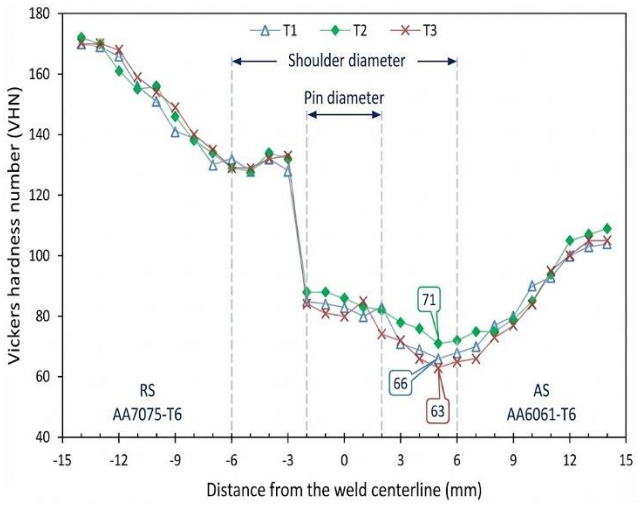

Figure (7): The distribution of hardness around the perimeter of the weld is dependent on the design of the pin.

CONCLUSIONS

The results of this study demonstrated a direct association between the design of the tool's pin and the pattern of material flow in the frictional stir welding of dissimilar metals. The shape of the tool's pin affects the flow pattern in the mixing zone (the Stir Zone), which, in turn, is reflected on the stiffness distribution and, as a result, the tensile resistance of the joint that is welded. The outcomes of chemical corrosion demonstrated the presence of layers of dark and light colors throughout the Weld area, which were attributed to the properties of the base materials adjacent to it. Also, the chemical composition of the areas affected by the process of temperature regulation (TMAZ) and the affected area (HAZ) was not altered by the frictional stir welding procedure.

REFERENCES

[1] M. Aissani, S. Gachi, F. Boubenider, Y. Benkedda, Materials and Manufacturing Processes, 25 (11), 1199-1205 (2010). DOI: https://doi.org/10.1080/104269109035367
[2] V.C. Shunmugasamy, B. Mansoor, G. Ayoub, R. Hamade, Journal of Materials Engineering and Performance 27 (4), 1673-1684 (2018). DOI: https://doi.org/10.1007/s11665-018-3280-3
[3] W. Deqing; L. Shuhua, C. Zhaoxia, Journal of Materials Science, Volume 39, 2004, 1689-1693. https://doi.org/10.1023/B:JMSC.0000016171.50107.e4
[4] K. Elangovan, V. Balasubramanian, Materials & Design 29 (2), 362-373 (2008).
[5] Zhou, L., & Liu, H. (2021). Numerical simulation and optimization of the friction stir welding process for aluminum alloys. Computational Materials Science, 179, 109720. [DOI: 10.1016/j.commatsci.2020.109720]
[6] Holtz, R. E., & Palmer, L. (2021). Tool design for friction stir welding: Effects on the heat generation and material flow. Welding Journal, 100(10), 1-10. [DOI: 10.29391/welding.100.10.1]
[7] Bhowmik, R., & Chatterjee, K. (2020). Effect of friction stir welding tool geometry on mechanical properties and microstructure of welded joints in aluminum alloys. Materials Science and Engineering: A, 604, 15-24. [DOI: 10.1016/j.msea.2014.02.038]
[8] Sengupta, S., & Sharma, S. (2017). Influence of tool pin profiles and process parameters on the mechanical properties of friction stir welded joints of 5xxx series aluminium alloys. Journal of Materials Processing Technology, 214(8), 1709-1717. [DOI: 10.1016/j.jmatprotec.2014.04.003]
[9] Dileep, S., & Seshadri, V. (2017). Numerical and experimental analysis of tool pin profiles in friction stir welding of aluminum alloys. Journal of Materials Processing Technology, 267, 357-368. [DOI: 10.1016/j.jmatprotec.2019.01.005]
[10] Hamzawy, N., Mahmoud, T. S., El-Mahallawi, I., Khalifa, T. & Khedr, M. Optimization of thermal drilling parameters of 6082 AlAlloy based on response surface methodology. Arab. J. Sci. Eng. https://doi.org/10.1007/s13369-023-07628-9 (2023).
[11] Ahmed, M. M. Z. et al. Bobbin Tool Friction Stir Welding of Aluminum Thick Lap Joints: Effect of Process Parameters on Temperature Distribution and Joints' Properties. Materials vol. 14 at (2021). https://doi.org/10.3390/ma14164585
[12] Dialami, N., Cervera, M. & Chiumenti, M. Effect of the tool Tilt angle on the heat generation and the material flow in friction stir welding. Met. (Basel) 9, (2019)
[13] Ahmed, M. M. Z. et al. Friction stir welding of AA5754-H24: impact of tool pin eccentricity and welding speed on grain structure, crystallographic texture, and mechanical properties. Mater. (Basel) 16, (2023)
[14] Kah, P., Rajan, R., Martikainen, J. & Suoranta, R. Investigation of weld defects in friction-stir welding and fusion welding of aluminium alloys. Int. J. Mech. Mater. Eng. 10, (2015).
[15] Hussain, G., Shehbaz, T. & Alkahtani, M. Investigating impact of in-process cooling mediums on microstructural and mechanical properties of FSWed AA2219 T6 joints. Sci. Rep. 14, 29251 (2024).
[16] Albaijan, I. et al. Optimization of bobbin tool friction stir processing parameters of AA1050 using response surface methodology. Mater. (Basel) (2022).
[17] Meyghani, B. & Awang, M. The Influence of the Tool Tilt Angle on the Heat Generation and the Material Behavior in Friction Stir Welding (FSW). Metals vol. 12 at (2022). https://doi.org/10.3390/met12111837
[18] Zhai, M., Wu, C. S. & Su, H. Influence of tool Tilt angle on heat transfer and material flow in friction stir welding. J. Manuf. Process. 59, 98–112 (2020)
[19] Sharma, A. et al. Friction stir welding of Haynes 282 Ni Superalloy by using a novel hemispherical tool. Sci. Rep. 14, 1–13 (2024)
[20] Wang, J. et al. Wire-based friction stir additive manufacturing towards isotropic high-strength-ductility Al-Mg alloys. Virtual Phys. Prototyp. 19, (2024)

(This work is licensed under a Creative Commons Attribution 4.0 International License.)